

The Malaysian International Tribology Conference 2013, MITC2013

Friction reduction in lubricated-MEMS with complex slip surface pattern

M. Tauviquirrahman^{a,b,*}, R. Ismail^{a,b}, J. Jamari^b, D.J. Schipper^a

^aLaboratory for Surface Technology and Tribology, Faculty of Engineering Technology, University of Twente
Drienerloolaan 5, Postbus 217, 7500 AE, Enschede, The Netherlands

^bLaboratory for Engineering Design and Tribology, Department of Mechanical Engineering, University of Diponegoro
Jl. Prof. Soedharto, Tembalang, Semarang, Indonesia

Abstract

Many types of micro-electro-mechanical-system (MEMS) based products are currently employed in a variety of applications. However, high friction in these systems is a problem which limits the development of MEMS devices in which sliding contacts are involved. The aim of this research is to evaluate the effect of boundary slip on the hydrodynamic friction in a low load lubricated MEMS, in particular when boundary slip takes places in the certain region of the lubricated sliding contact, i.e. complex slip surface pattern. The effectiveness of the boundary slip in reducing friction is highlighted. The results indicate that the deterministic complex slip pattern has a beneficial effect on decreasing friction.

© 2013 The Authors. Published by Elsevier Ltd. Open access under [CC BY-NC-ND license](https://creativecommons.org/licenses/by-nc-nd/4.0/).

Selection and peer-review under responsibility of The Malaysian Tribology Society (MYTRIBOS), Department of Mechanical Engineering, Universiti Malaya, 50603 Kuala Lumpur, Malaysia

Keywords: Boundary slip; Friction; Lubrication; Micro-electro-mechanical-system (MEMS).

Nomenclature

h	film thickness (m)
f	friction force (N)
l_s	length of the slip zone (m)
p	pressure (Pa)
U	sliding velocity (m/s)
<i>Greek symbols</i>	
α_a, α_b	slip coefficient (m ² /s/kg)
β	slip length (m)
η	dynamic viscosity (Pa.s)

* Corresponding author. Tel.: +62-24-7460059 ext 115; fax: +62-24-7460059 ext 102.
E-mail address: mtauviq99@gmail.com

μ	coefficient of friction
τ_{xz}	shear stress (Pa)
<i>Subscripts</i>	
i, o	inlet, outlet
a, b	top, bottom

1. Introduction

For the last years, there has been a tremendous effort towards the development of micro-electro-mechanical-system (MEMS) for a wide variety of applications. However, one main factor that limits the widespread development and reliability of MEMS is a high level of friction and wear [1]. Furthermore, every type of MEMS device is susceptible to stiction [2]. Stiction (a subtraction of ‘static friction’) in micro-system technology has been still a problem which limits the life-time of MEMS devices. As the overall size of a device is reduced, the capillary and surface tension forces of the liquid become large, which induce stiction rendering the devices to fail or malfunction.

Several approaches to address the stiction between two opposing surfaces have been proposed including self-assembled molecular (SAM) coatings, hermetic packaging and the use of reactive materials in the package [3]. Another promising technique to tackle the stiction problem is by using a liquid lubricant between the interacting components of MEMS devices, with high amounts of sliding. However, a significant barrier in the development of MEMS lubrication is the problem of achieving proper tribological performance of their moving parts [4], because the lubricant behavior is different at micro-scale compared to macro-scale. In the classical lubrication theory, it is well-known that the no-slip boundary condition, i.e. the fluid is immediately adjacent to a solid surface and moves at the same velocity as the surface, is the core concept [5]. The no-slip boundary has been employed almost universally at macroscopic level in the fluid mechanics and remains an assumption that is not based on physical principles. However, with the continuous progress of the measurement techniques during recent years, strong evidence for slip has been provided by a great number of researchers [6-13]. The evidence of slip has been generally accepted and for certain cases the no-slip boundary condition is not valid. In lubricated-MEMS, the no-slip boundary is generally an unwanted condition because it can lead to the occurrence of stiction and as a result the micro-parts cannot move [2].

In liquid lubricated-MEMS, the boundary condition will play a very important role in determining the lubricant flow behavior. A technique of controlling the hydrodynamic friction is to promote the occurrence of boundary slip at the surface. In published works [11-15], both experimentally and numerically, it was shown that boundary slip is able to reduce hydrodynamic friction at the contacting surfaces. These findings allow the use of liquid lubrication in MEMS become feasible in practice. Further, in recent work [16] the effectiveness of boundary slip in a deterministic way was investigated with respect to load support. The authors proposed the so-called complex slip surface (CSS) pattern. The stationary surface was modified in such a way that boundary slip takes places in the certain region. The complex slip surface predicted the improvement of the load support significantly. This paper focuses on the feasibility of CSS pattern in generating a low friction in lubricated MEMS.

2. Mathematical model

The classical Reynolds equation that is valid under no-slip boundary condition can be generalized taking into account boundary slip. It is then possible, for any film thickness height distributions, to calculate the hydrodynamic pressure and the shear rate distributions. The model of lubrication presented here is based on the fact that slip of the lubricant will exist at the interface between a lubricant and solid surface in a lubricated sliding contact. Boundary slip is employed both on the moving and stationary surface, see Fig. 1. The lubrication model with slip leads to a modified Reynolds equation as presented in Eq. (1), see Ref. [16] for the derivation. In this study, it should be noted that the occurrence of slip in a lubricated sliding contact is determined by two criteria. Firstly, slip may only occur in those areas where both stationary and moving surface have been treated to allow it. Secondly, the shear stress on both surfaces must exceed a critical shear stress value, referred as τ_{ca} for stationary surface and τ_{cb} for the moving surface. When both criteria are met the resulting slip velocity is proportional to the difference between the shear

stress and the critical value, with proportionality factors referred to as α_a for the stationary surface and α_b for the moving surface. It means that each of the surfaces has a unique slip property. The product of the slip coefficient with the viscosity, $\alpha\eta$, is commonly named ‘slip length’.

Eq. (1) is derived by following the usual approach to deduce the Reynolds equation from the Navier-Stokes system by assuming classical assumptions except that boundary slip is applied both on the stationary surface and the moving surface as depicted in Fig. 1.

$$\begin{aligned} \frac{\partial}{\partial x} \left(h^3 \frac{h^2 + 4h\eta(\alpha_a + \alpha_b) + 12\eta^2 \alpha_a \alpha_b}{h(h + \eta(\alpha_a + \alpha_b))} \frac{\partial p}{\partial x} \right) &= 6\eta U \frac{\partial}{\partial x} \left(\frac{h^2 + 2h\alpha_a \eta}{h + \eta(\alpha_a + \alpha_b)} \right) \\ -6\eta \tau_{ca} \frac{\partial}{\partial x} \left(\frac{\alpha_a h(h + 2\alpha_a \eta)}{h + \eta(\alpha_a + \alpha_b)} \right) + 6\eta \tau_{cb} \frac{\partial}{\partial x} \left(\frac{\alpha_b h(h + 2\alpha_b \eta)}{h + \eta(\alpha_a + \alpha_b)} \right) - 12\eta U \frac{\alpha_a \eta}{h + \eta(\alpha_a + \alpha_b)} \frac{\partial h}{\partial x} \\ \frac{\partial}{\partial x} \left(h^3 \frac{h^2 + 4h\eta(\alpha_a + \alpha_b) + 12\eta^2 \alpha_a \alpha_b}{h(h + \eta(\alpha_a + \alpha_b))} \frac{\partial p}{\partial x} \right) &= 6\eta U \frac{\partial}{\partial x} \left(\frac{h^2 + 2h\alpha_a \eta}{h + \eta(\alpha_a + \alpha_b)} \right) \end{aligned} \quad (1)$$

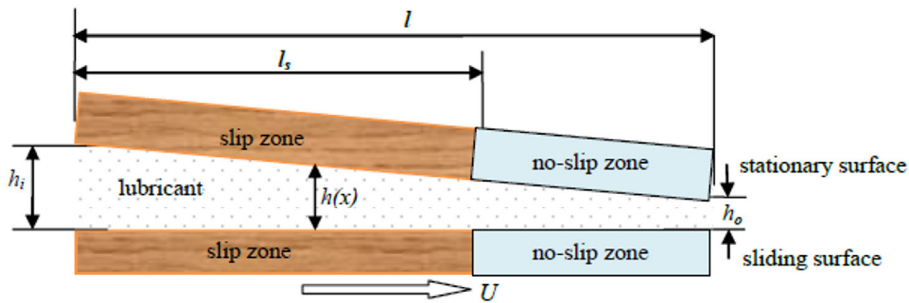


Fig. 1. Schematic representation of lubricated sliding MEMS contact with artificial slip zone.

3. Numerical procedure

The modified Reynolds equation, Eq. (1) is solved numerically using finite difference equations obtained by means of the micro-control volume approach and using the Tri-diagonal-Matrix-Algorithm (TDMA), [17]. By employing the discretization scheme, the computed domain is divided into a number of control volumes using a grid with uniform mesh size which is applied to the slip region. 101 meshes are employed in the computational domain. The grid independency is validated by changing the mesh size. If the mesh number was above 101, the simulation results did not differ anymore. But obviously the computational cost increased.

To investigate the effect of boundary slip characteristics on the lubrication performance of sliding surfaces, various parameters are set. The primary parameters for all following computations are given as follows: sliding velocity U is 1 m/s (the corresponding Reynolds number Re is 1 assuming the fluid density is 1,000 kg/m³ and the dynamic viscosity η is 0.001 Pa.s), the total length of the lubricated contact l is 20×10^{-3} m and the outlet film thickness h_o is 1×10^{-6} m. In the following simulations, the slip coefficient α varies from 0 to 0.05 m²/kg based on the results published in literature [11, 12, 15, 18]. All parameters and the range in which they are varied are summarized in Table 1. An assumption is made that the boundary pressures are zero at both sides of the contact. In

the present study, Reynolds boundary cavitation condition is modeled. It consists in ensuring that $p = 0$ and $\partial p / \partial x = 0$ at the rupture limits of the lubricant film. The most important parameters such as dimensionless slip length B (where $B = \eta\alpha/h_o$) and slope incline ratio H (where $H = h_i/h_o$) are examined in detail.

Table 1. Simulated parameters

Parameter	Data setting	Unit
Slip coefficient, α	0-0.05	$\text{m}^2 \cdot \text{s} / \text{kg}$
Slope incline ratio, H	1-3	[-]

4. Results

4.1. Effect of slope incline ratio

The hydrodynamic viscous friction force is a good measure for determining the effectiveness of the deterministic boundary slip. The friction force of a lubrication film can be achieved by integrating the shear stress over the surface area. The simulation results will be presented in dimensionless form, i.e. $F = fh_o/(U\eta l)$ for dimensionless friction force in which f is friction force per unit width and $T_{xz} = \tau_{xz}h_o/(U\eta)$ for dimensionless local shear stress.

Previous research [16] demonstrated that a complex slip surface (CSS) is superior to a homogeneous slip surface as well as no-slip surface with respect to load support. The CSS pattern is generally most effective with respect to the maximum load support if (1) the length of the slip zone l_s of complex slip surface (CSS) covers 0.65 of the contact length l at the leading edge of the contact, see Fig. 1, (2) the critical shear stress τ_c is zero, and/or (3) slip is applied only on the stationary surface. In the present study, in order to show the benefit of the use of a CSS pattern, all slip profiles are compared with the no-slip distribution at the optimized slope incline ratio H of 2.2. From the analytical solution described in Ref. [19], it is known that at H of 2.2, the hydrodynamic pressure has the highest value. In the following computations, the CSS properties $l_s/l = 0.65$ and $\tau_c = 0$ are employed on the stationary surface.

Figure 2a shows the dimensionless surface shear stress distribution T_{xz} for different values of several slope incline ratio H as a function of dimensionless coordinate x/l . It can be seen that for all H , the dimensionless shear stress distribution is mainly higher in the region of slip, compared to the contact region with no slip surface, but decreases considerably in the region of no slip, compared to the contact region with no slip surface. As is shown in Fig. 2b, when $H = 1$ (i.e. parallel sliding surfaces), the minimum dimensionless friction force is highlighted. This finding is very beneficial with respect to the tribological performance, because as discussed in Ref. [16], the optimized CSS pattern (i.e. $l_s/l = 0.65$) with parallel sliding surfaces gives the highest load support. From Fig. 2b, it is also found that when compared with the no slip case at the same H , the friction predicted by CSS pattern is much lower especially for very low H . This is to say, that in addition to the improvement of the load support [16], the use of CSS pattern is also effective for reducing the friction even the absence of the wedge effect (i.e. parallel sliding surfaces).

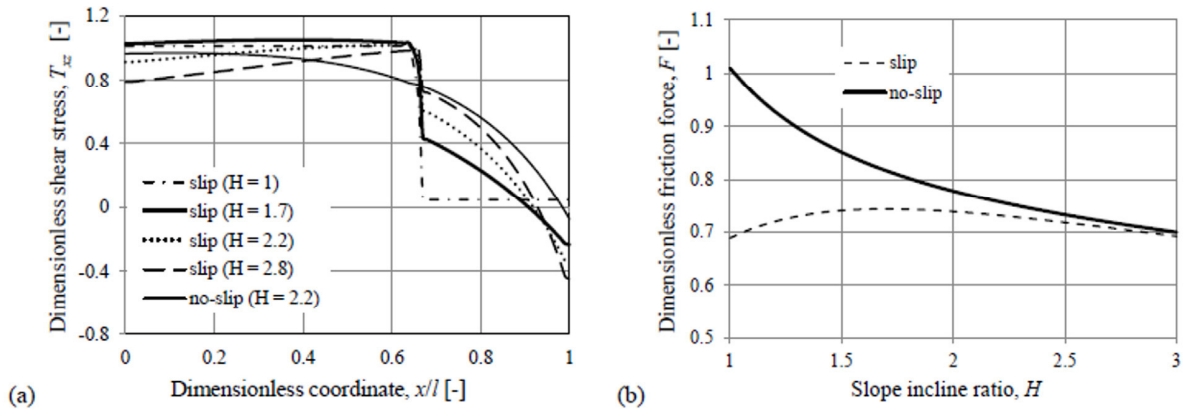


Fig. 2. (a) Distribution of dimensionless shear stress T_{xz} for several slope incline ratio H , (b) Dimensionless friction force F as a function of the slope incline ratio H . All slip profiles are calculated for dimensionless slip length B of 20.

4.2. Effect of slip length

All slip profiles presented in Fig. 2 are predicted using the dimensionless slip length B of 20. Therefore, the issue of how does the dimensionless slip length affect the friction force for the CSS pattern will be explored in this section. The variation of the dimensionless friction force F as a function of the dimensionless slip length B for various slope incline ratio values H is shown in Fig. 3a. Generally, for all H it appears that dimensionless friction force will decrease with an increase in the dimensionless slip length B , especially for small B . However, only for cases with high H ($H > 2.2$), a significant friction reduction is not found. For example, for the CSS pattern subject to a dimensionless slip length of 50, the friction force differs from the no-slip surface (i.e. when $B = 0$) by only 1.3 % (lower). As the slope incline ratio is decreased to 1 (i.e. parallel sliding surfaces), the discrepancies in friction force increases (at a dimensionless slip length of 50, it is up 32%). It means that the beneficial effect of CSS will vanish with respect to friction due to the wedge effect (dh/dx). This result, again, strengthens the previous finding (see Fig. 2) which mentioned that only when the wedge effect is absent (i.e. $H = 1$), the friction reaches a minimum value and this is the most wanted effect in lubricated MEMS.

Inspection of Fig. 3a shows that in the case of parallel sliding surface ($H = 1$), when the dimensionless slip length B is smaller than 10, the friction decreases significantly. The reduction in hydrodynamic friction has mainly been attributed to the decrease in the shear stress distribution in the no slip region with the increase of slip length (see Fig. 3b). It can also be deduced from Fig. 3a that after $B = 10$, increasing the slip zone will be less effective to reduce friction. Here, the dimensionless slip length B of 10 can be considered as an optimal value for generating a perfect slip effect in the lubricated sliding contacts. However, for a higher value of H (for example $H = 2.8$), there is a shift of the optimum dimensionless slip length towards the B value which is smaller than the optimum of B for the case of $H = 1$, i.e somewhere between $B = 1$ and $B = 3$. It indicates that there is a threshold value of the dimensionless slip length which is unique for each slope incline ratio. In general, however, the best characteristic performance can be achieved when the configuration of the CSS pattern has a high slip length. This is as expected because a large value of slip length implies larger boundary slip. This has also been confirmed in recent literature [20, 21].

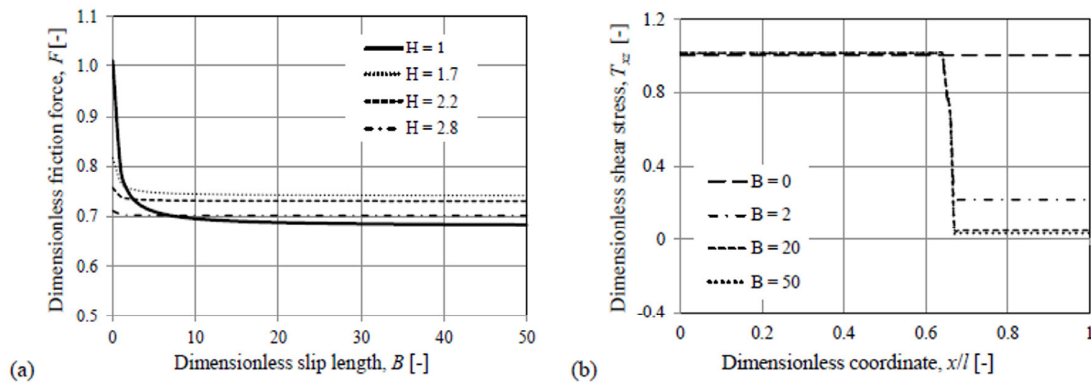


Fig. 3. (a) Dimensionless friction force F as a function of dimensionless slip length B with different values of slope incline ratio H , (b) Distribution of dimensionless shear stress T_{xz} for several dimensionless slip lengths B in the case of parallel sliding surfaces.

5. Discussions

In a real system, for example in lubricated-MEMS containing moving surfaces, the complex slip surface (CSS) pattern can be a promising way for increasing the load support and reducing the friction. Because a CSS pattern is relatively easy to obtain, the CSS pattern for increased-MEMS performance by lubrication may be more applicable. If compared to the use of texturing which needs the technology of texturing (for instance using a laser), the slip zone can be obtained by grafting or by the deposition of hydrophobic compounds to the initial surfaces. These technical procedures can lead to a modification of the surface energy [22], i.e. wettability.

The CSS pattern may consist of the combination of two surface types, i.e. hydrophilic and hydrophobic. They can lead to a method to control boundary slip. A (super) hydrophobic surface shows boundary slip compared to hydrophilic surfaces. For most hydrophilic surfaces, no-slip occurs [23]. As is well-known, MEMS technology frequently exhibits parallel moving surfaces. In such a surface, with a homogeneous slip and/or no-slip condition, no load support takes place [15, 16]. Based on the numerical simulations presented here, even the absence of the wedge effect, it was shown that an optimized complex slip surface (CSS) pattern leads to better performance in terms of friction reduction.

6. Conclusions

In the present study, numerical efforts of exploring boundary slip in a deterministic way (i.e. complex slip surface (CSS) pattern) in obtaining a low friction were of particular interest. The modified Reynolds equation has been used to evaluate the effects of CSS pattern in lubricated-MEMS. The results indicated that the deterministic complex slip pattern has a beneficial effect by decreasing the friction. Practical recommendation on the importance of the well-chosen operational parameter was given. A high slip length and low slope incline ratio were found to be positive in terms of friction reduction for the flow condition studied. In general, it is very beneficial to make one of the contacting surfaces in lubricated-MEMS with a CSS pattern surface for achieving an ideal lubrication performance, i.e. reduced friction.

References

- [1] Henck, S.A., 1997. Lubrication of Digital Micromirror Devices, *Tribology Letters* 3, p. 239.
- [2] Israelachvili J., 1995. *Intermolecular and Surface Force* vol. 1. 2nd edition, Academic Press, London.
- [3] van Spengen, W.M., Puers, R., De Wolf, 2003. On the Physics of Stiction and Its Impact on the Reliability of Microstructures, *Journal of Adhesion Science and Technology* 17, p. 563.

- [4] Spearing, S.M., 2000. Materials Issues in Microelectromechanical systems (MEMS), *Acta Materialia* 48, p. 179.
- [5] Hamrock, B.J., 1994. *Fundamentals of Fluid Film Lubrication*, McGraw-Hill, Inc., New York.
- [6] Zhu, Y., Granick, S., 2001. Rate Dependent Slip of Newtonian Liquid at Smooth Surfaces, *Physical Review Letters* 87, p. 096105.
- [7] Spikes, H.A., Granick, S., 2003. Equation for Slip of Simple Liquids at Smooth Solid Surfaces, *Langmuir* 19, p. 5065.
- [8] Zhu, Y., Granick, S., 2002. Limits of Hydrodynamic No-Slip Boundary Condition, *Physical Review Letters* 88, p. 106102.
- [9] Hild, W., Opitz, A., Schaefer, J.A., Scherge, M., 2003. The Effect of Wetting on the Microhydrodynamics of Surfaces Lubricated With Water and Oil, *Wear* 254, p. 871.
- [10] Cheng, J.-T., Giordano, N., 2002. Fluid Flow Through Nanometer-Scale Channels, *Physical Review E* 65, p. 031206.
- [11] Choo, J.H., Spikes, H.A., Ratoi, M., Glovnea, R., Forrest, A., 2007. Friction Reduction in Low-load Hydrodynamic Lubrication with a Hydrophobic Surface, *Tribology International* 40, p. 154.
- [12] Choo, J.H., Glovnea, R.P., Forrest, A.K., Spikes, H.A., 2007. A Low Friction Bearing Based on Liquid Slip at the Wall, *ASME Journal of Tribology* 129, p. 611.
- [13] Leong, J.Y., Reddyhoff, T., Sinha, S.K., Holmes, A.S., Spikes, H.A., 2013. Hydrodynamic Friction Reduction in a MAC-Hexadecane Lubricated MEMS Contact, *Tribology Letters* 49, p. 217.
- [14] Spikes, H.A., 2003, The Half-Wetted Bearing. Part I: Extended Reynolds Equation, *Proceedings of the Institution of Mechanical Engineers, Part J: Journal of Engineering Tribology* 217, p. 1.
- [15] Salant, R.F., Fortier, A.E., 2004, Numerical Analysis of a Slider Bearing with a Heterogeneous Slip/No-Slip Surface, *Tribology Transactions* 47, p. 328.
- [16] Tauviquirrahman, M., Ismail, R., Jamari, J., Schipper, D.J., 2013. Study of Surface Texturing and Boundary Slip on Improving the Load Support of Lubricated Sliding Contacts, *Acta Mechanica* 224, p. 365.
- [17] Patankar, S.V., 1980. *Numerical heat transfer and fluid flow*, Taylor & Francis, Levittown.
- [18] Watanabe, K., Yanuar, Udagawa, H., 1999. Drag Reduction of Newtonian Fluid in a Circular Pipe with a Highly Water-Repellent Wall, *Journal of Fluid Mechanics* 381, p. 225.
- [19] Cameron, A., 1966. *The principles of Lubrication*, Longman Green and Co,Ltd, London.
- [20] Rao, T.V.V.L.N., Rani, A.M.A., Nagarajan, T., Hashim, F.M., 2012. Analysis of Slider and Journal Bearing using Partially Textured Slip Surface, *Tribology International* 56, p. 121.
- [21] Wang, L.L., Lu, C.H., Wang, M., Fu, W.X., 2012. The Numerical Analysis of the Radial Sleeve Bearing with Combined Surface Slip, *Tribology International* 47, p. 100.
- [22] Aurelian, F., Patrick, M., Mohamed, H., 2011. Wall Slip Effects in (Elasto) Hydrodynamic Journal Bearing, *Tribology International* 44, p. 868.
- [23] Wu, C.W., Ma, G.J., Zhou, P., 2006. Low Friction and High Load Support Capacity of Slider Bearing with a Mixed Slip Surface, *ASME Journal of Tribology* 128, p. 904.